ELSEVIER

Biochimica et Biophysica Acta 1514 (2001) 87–99

BIOCHIMICA ET BIOPHYSICA ACTA
BBA

www.bba-direct.com

Transduction to self-assembly of molecular geometry and local interactions in mixtures of ceramides and ganglioside GM1

Dolores C. Carrer, Bruno Maggio *

Departamento de Química Biológica – CIQUIBIC, Facultad de Ciencias Químicas – CONICET, Universidad Nacional de Córdoba, Ciudad Universitaria, 5000 Córdoba, Argentina

Received 3 May 2001; received in revised form 18 June 2001; accepted 20 June 2001

Abstract

In mixed monolayers with ganglioside GM1, ceramide induces a non-ideal increase of the monolayer collapse pressure, a reduction of the mean molecular area and a decrease of the surface potential per molecule at all surface pressures. The critical packing parameter and van der Waals interaction energy calculated from monolayer data predict the transduction of changes from the molecular to the supramolecular level, such as formation of bilayers and possible subsequent facilitation of non-bilayer structures as the ceramide concentration increases, along with a greater thermal stability of the lipid structures. In agreement with the expectations from monolayer data, calorimetry, dynamic light scattering and electron microscopy data reveal the actual presence of phases with high phase-transition temperatures; at about 5 mol% ceramide in the mixture, the aggregates change their topology from micelles to multilamellar vesicles of increasing size and finally to long, thin tubules as the amount of ceramide in the system increases.

Keywords: Ceramide; Ganglioside; Calorimetry; Monolayer; Dynamic light scattering; Glycolipid self assembly

1. Introduction

Ceramide (Cer) constitutes a pivotal structural, metabolic and functional membrane component that can participate in transduction pathways regulating a variety of cellular events [1,2]. Also, Cer is the initial and final step for the metabolism of complex neutral glycosphingolipids and gangliosides that are, by themselves, important biomodulators of the structural and functional dynamics of biomembranes [3,4].These sphingolipids are enriched in localized regions of the cell plasma membrane which have been increasingly implicated in playing a role as compartmentalized signal transduction domains that also contain other membrane lipids and protein-coupled receptors [5].

However, information on the effect of Cer and other complex sphingolipids on the dynamic organization of biomembranes is scarce and an integrated view at the molecular level of their functional role is not yet possible although studies have been increasingly reported. These refer to changes of the molecular packing and surface electrostatics and phase state induced by Cer [6,7] and several individual glycosphingolipids, including systems containing different phospholipids [4]. It was previously demonstrated

Abbreviations: Cer, Ceramide (*N*-acyl sphingoid); Ganglioside GM1, Galβ1–3GalNAcβ1–4Gal(3–2αNeuAc) β1–4Glcβ1–1Cer; ΔH_{cal}, calorimetric enthalpy; T_m, temperature corresponding to the maximum excess heat capacity ΔC_{pmax}; DSC, differential scanning calorimetry

* Corresponding author. Fax: +54-351-433-4074.

E-mail address: bmaggio@dqbfcq.uncor.edu (B. Maggio).

0005-2736/01/$ – see front matter
PII: S0005-2736(01)00366-2

by systematic studies on a series of chemically related sphingolipids that those effects depended markedly on the type of polar head group present in the sphingolipid [4]. Directly or indirectly, this also has a profound modulatory influence on interactions with integral and extrinsic proteins [4,8,9], intermembrane interactions [10] and phosphohydrolytic activity [11].

Another important feature in sphingolipids is that the type and complexity of their polar head group in relation to the acylated sphingosine moiety to which it is linked can determine markedly different molecular geometries [4,12] with a dramatic transduction to the topology of the self-assembled structure adopted in aqueous media [13]. The geometrical form of an individual molecule is expressed in a dimensionless packing parameter ($P_c = v/a_o l_c$) defined by the optimum area at the hydrophobic–hydrophilic interface (a_o) and the length (l_c) and volume (v) of the hydrophobic portion [14]. In turn, critical values for P_c determine the overall shape and interfacial curvature of the self-aggregated structure. This is due to the balance and interplay of simultaneous constraints imposed by different intrinsic molecular geometries, interaction free energies, entropy and viscoelastic relaxation of the combined tensions through deformation and curvature [12–15].

Either for individual sphingolipids or for more complex mixtures with other lipids the above synergic effects determine the adoption of a rich variety of shapes, sizes and curvature of the structures formed [13]. This includes facilitation or hindrance for formation of non-bilayer phases [16], and modulation of these topological features can be achieved by relatively small changes of the proportions of gangliosides, phospholipids, cholesterol and ceramide [17–20]. It is now clear that subtle compensations of the molecular geometry and local curvature in lipid mixtures is at the basis of effects taking place at a supramolecular level of the membrane as amplified responses [4]. Such structural effect of these sphingolipids have already been shown to induce marked alterations of the activity of phosphohydrolytic enzymes that generate lipid second messengers and the susceptibility of lipid bilayers to recombination and fusion [10,11,21–23].

The aim of the present work was to investigate changes of intermolecular interactions and the thermodynamic and geometrical interplay taking place in mixtures of two sphingolipids that are situated at two extremes of the series in terms of their molecular packing, individual geometry, phase state and self assembled topology [4,12,13] such as Cer (closely packed, liquid condensed, high T_m, $P_c > 1$, inverted cone with negative curvature, H_{II}(inverted micelle)-phase forming lipid) and ganglioside GM1 (loosely packed, liquid expanded, low T_m, $P_c < 0.5$, straight cone with positive curvature, H_I(micelle)-phase forming lipid).

2. Experimental procedures

2.1. Materials

Bovine brain ceramide (type III) from Sigma–Aldrich (St. Louis, MO), contains primarily (over 82%) stearic (18:0) and nervonic (15-tetracosenoic) fatty acids. Ganglioside GM1 was obtained from bovine brain though a purification procedure previously described [24]; about 85% of the sphingosine-linked fatty acids was represented by stearic, arachidic and nervonic acids, the sphingosine base composition was mostly (over 82%) 18:1 and 20:1 sphingosine (4-sphingenine). Both lipids were over 99% pure according to high-performance thin-layer chromatography [6,24]. Solvents were of the highest purity available from Merck (Darmstadt, Germany). Water was double-distilled in an all-glass apparatus.

2.2. Lipid monolayers

Monolayers were spread from premixed solutions in chloroform/methanol (2:1) for Cer and chloroform/methanol/water (2:1:0.15) for GM1; details of the techniques and equipment used were given in previous publications [6,11,25]. Absence of surface-active impurities in the subphase and in the spreading solvents was routinely controlled as described [11]. Surface pressure- and surface potential- vs. molecular area isotherms were obtained at 25°C by spreading less than 15 μl of lipid solution on the surface of NaCl 145 mM solution contained in one of the compartments (90 cm^2) of a specially designed circular Teflon-coated trough of a Monofilmmeter (Mayer Feintechnik, Germany) with a platinized-Pt

sensing plate connected to a surface pressure transducer; surface potential was measured by a high impedance millivoltmeter (Corning ionalyzer 250) connected to a surface ionizing electrode formed by an ^{241}Am plate positioned 5 mm above the monolayer surface, and to a reference calomel electrode connected to the aqueous subphase through a saline bridge [11]. Temperature was maintained within ±0.3°C with a refrigerated Haake F3C thermocirculator. Duplicate and triplicate monolayer isotherms were obtained at a compression rate of 45–60 Å^2 molecule^{-1} min^{-1} and averaged; reducing further the compression speed produced no change in the isotherms. Reproducibility was within maximum S.E.M. of ±1 mN/m for surface pressure, ±20 mV for surface potential, and ±2 Å^2 for molecular areas.

2.3. Aqueous lipid dispersions

Lipids were premixed in the desired proportions from solutions prepared in chloroform/methanol (2:1). The mixture was taken to dryness as a thin film in a conical bottom tube under a stream of N_2 and submitted to vacuum for at least 4 h. The dry lipid was hydrated (at a final concentration between 7.0 and 16.6 mM) with NaCl 145 mM in double-distilled filtered water and submitted to freeze–thaw cycles of 5 min at least four times between −180°C and 90°C [26]; lipid dispersions were formed by vigorous vortexing above 70°C.

2.4. Calorimetry

The dispersion was introduced, after degassing under reduced pressure, into the sample cell of a MC2D-Microcal high sensitivity differential scanning calorimeter (Microcal, Amherst, MA) with the reference cell filled with 145 mM NaCl. The proportions of Cer with respect to GM1 varied between 0 and 33 mol%, the amount of total lipid was between 7.0 and 16.6 mM. Samples were scanned at 30°C/h, duplicate or triplicate runs for each condition were performed and the scans were normalized [6].

2.5. Dynamic light scattering

Aqueous lipid dispersions were introduced into the thermostatized sample cell of a Nicomp Model 380 Submicron Particle Sizer (PSS, CA, USA) and measured at 23°C before and after the same sample was submitted to calorimetry (average time lapse: 20 h). Each sample was measured at least four times. The data were collected and analyzed with the software provided with the instrument.

2.6. Electron microscopy

Aqueous lipid dispersions (3–7 mg/ml) were prepared as described above. Two percent sodium phosphotungstate or uranyl acetate were used as negative staining solutions. Three hundred mesh copper electron microscope grids coated with colodion holey film and evaporated carbon were used as support. Observations were made with a JEM 1200EXII-JEOL electronic transmission microscope (Japan) operating at 80 kV.

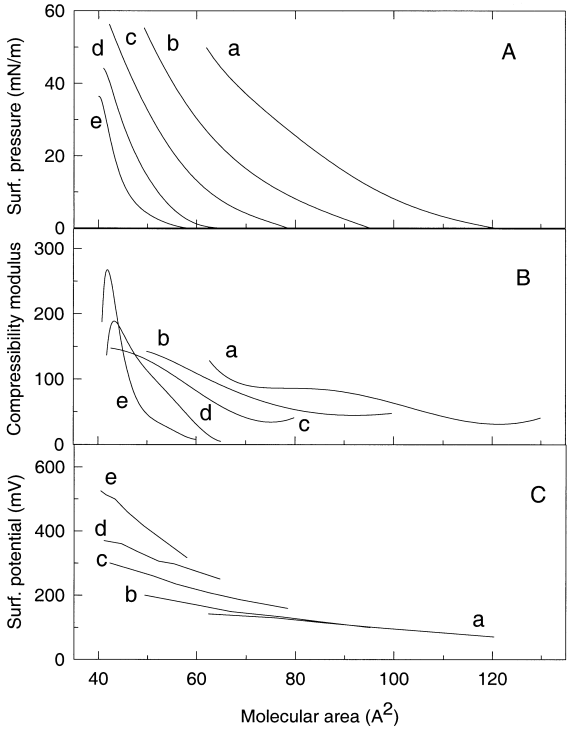

Fig. 1. Surface pressure, compressibility modulus and surface potential in mixed monolayers of Cer and GM1. Variation of surface pressure (A), compressibility modulus (B) and surface potential (C) with molecular area for GM1 (a), GM1/Cer (3:1) (b), GM1/Cer (1:1) (c), GM1/Cer (1:3) (d) and Cer (e).

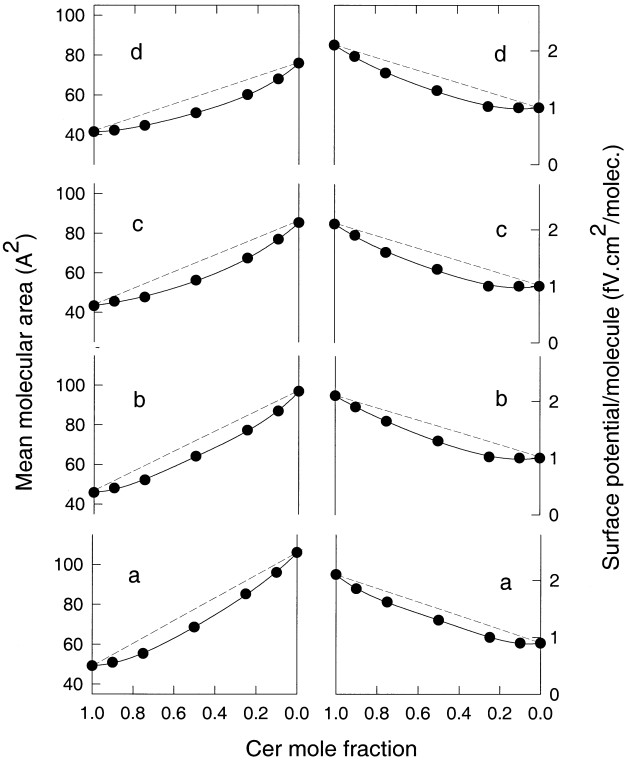

Fig. 2. Deviation of real mixed monolayer behavior from ideal behavior. Variation of mean molecular area and surface potential per molecule with Cer mole fraction at lateral pressures of 5 mN/m (a), 10 mN/m (b), 20 mN/m (c) and 30 mN/m (d).

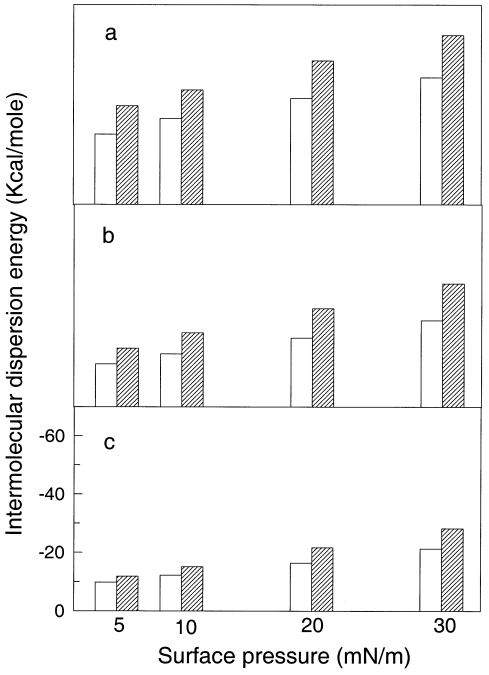

Fig. 3. Intermolecular dispersion energies in mixed monolayers. Intermolecular dispersion energy (van der Waals energy) vs. surface pressure of GM1/Cer (1:3) (a), GM1/Cer (1:1) (b) and GM1/Cer (3:1) (c) in ideal (white) and real (cross-hatched) mixtures.

3. Results

3.1. Cer–GM1 interactions in mixed lipid monolayers

Fig. 1 shows the variation of the surface pressure and surface potential with the mean molecular area for mixed films of Cer and ganglioside GM1 in different proportions. Intermolecular interactions occur in the mixed monolayers that lead to a closer than expected intermolecular packing areas and a reduced molecular polarization, as evidenced by the negative deviations from the additivity rule corresponding to ideal mixtures for both the mean molecular areas and the mean surface potential per unit of molecular surface density (usually denominated surface potential/molecule) at all surface pressures (Fig. 2).

Fig. 3 shows the intermolecular dispersion energy (calculated with Salem's equation [27,28]) for ideal and real mixtures of Cer/GM1 in different proportions. The increased condensation of the mean mo-

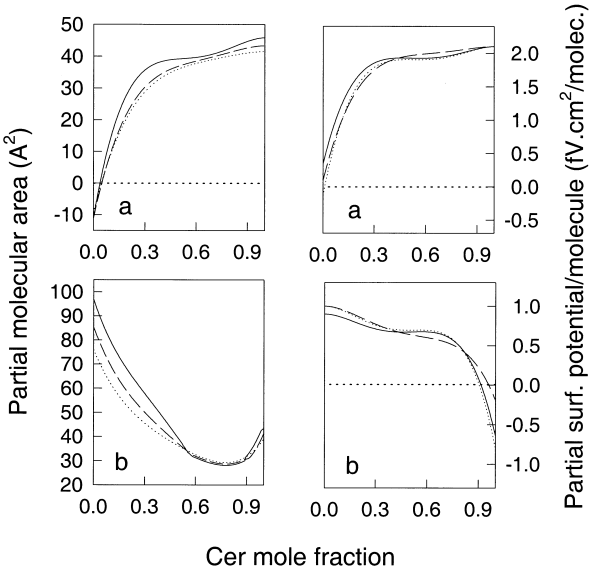

Fig. 4. Partial molecular parameters in mixed monolayers. Partial molecular area and partial surface potential per molecule for Cer (a) and GM1 (b) as a function of Cer mole fraction in the monolayer. Results are shown at 10 mN/m (full line), 20 mN/m (dashed line) and 30 mN/m (dotted line).

lecular area taking place in the real mixture compared to that expected in ideally mixed films leads to increases of the cohesive intermolecular energies at all values of surface pressure.

Calculations of the partial molecular areas (method of intercepts, [29]) occupied by Cer or by GM1 in the mixed films at different mole fractions indicate that GM1 is progressively condensed by Cer starting at low proportions of the latter (Fig. 4b) up to about 60 mol% of Cer in the mixture; the packing of GM1 can probably not be reduced further than about the minimum cross sectional area of two closely packed parallel hydrocarbon chains (30–40 $Å^2$) [30]. The change of the monolayer phase state by the condensing effect of increasing proportions of Cer is also evident from the values of the surface compressibility modulus [6] in the mixed films enriched in Cer (Fig. 1B). On the other hand, the molecular packing of Cer in the mixed film remains largely unchanged up to mole fractions of GM1 above about 0.8. Beyond this point it apparently packs into smaller molecular areas (Fig. 4a) than those expected for its own two hydrocarbon chains at the closest packing (about 38 ± 2 $Å^2$) and even takes negative values at higher proportions of GM1.

The individual molecular dipoles of each sphingolipid in the mixed films appears to be insensitive to alterations except at compositions highly enriched in either lipid (above about 80 mol%) where they undergo marked depolarization (Fig. 4).

3.2. Calorimetry and light scattering

As described in detail previously [6] pure Cer cannot be properly hydrated and does not form well dispersed mesophases in excess aqueous solutions that could be homogeneously introduced into the liquid sample cell available in our calorimeter. From monolayer experiments at different temperatures it was previously estimated that a bulk phase transition temperature of Cer should occur at about 80°C [31]; this is in reasonable agreement with metastable transitions reported in the 70–100°C range for dry and partially hydrated samples of Cer that were quite concentrated in terms of lipid mass [32].

The type and complexity of the polar head group in sphingolipids and gangliosides is of paramount importance for determining their optimum cross-sectional area at the hydrophobic–hydrophilic interface [4], the thermotropic behavior for the individual lipids and for their mixtures with phospholipids [4,9,26], as well as their organization into self-assembled structures in aqueous dispersions [12,13]. For gangliosides, it was previously emphasized that a careful purification procedure is required in order to obtain reliable description of their molecular behavior; this is due to variable amounts of peptides and acidic phosphatides that remain with gangliosides throughout standard purification procedures and to processes of internal lactonization in the ganglioside oligosaccharide chain occurring in stored solutions [24].

The complex hydration process in gangliosides and other sphingolipids requires preliminary cycling between low and high temperatures in order to obtain reproducible calorimetric measurements [6,26]. However, even with these precautions gangliosides can exhibit a temperature-dependent structural rearrangement of their preferred aggregated state in aqueous solutions. This was mostly ascribed to changes in the conformation and/or hydration of the oligosaccharide chain depending on temperature thresholds above 50–60°C [33,34]. Other authors using commercial GM1 ascribed the temperature-induced changes of aggregation properties to solubility effects [35]. Fig. 5A,B confirm that GM1 undergoes a temperature-induced conversion of its aggregated state that are reflected in variations of the thermotropic behavior. After 3–5 freezing and thawing cycles a solution of GM1 shows a narrow distribution of sizes with an average diameter of 13 ± 2 nm (Fig. 5Ba), in general agreement with previous measurements [13]. When run a first time between 5°C and 95°C in the calorimeter this preparation showed a low enthalpy ($\Delta H_{cal} \approx 0.8$ kcal/mol) broad transition characteristic of micellar aggregates (cf. [26]) centered at about 20°C (Fig. 5Aa). When cooled to 3°C and run immediately a second time the transition shifted to a lower T_m of about 15°C with a diminished enthalpy (Fig. 5Aa). The size distribution of the sample after having been run twice was still narrow but the average diameter had decreased to 10.6 ± 1.6 nm (Fig. 5Ba). The average diameter of a sample that was not run but was kept for 24 h at room temperature was not modified, and in general for all samples, no changes in light scatter measure-

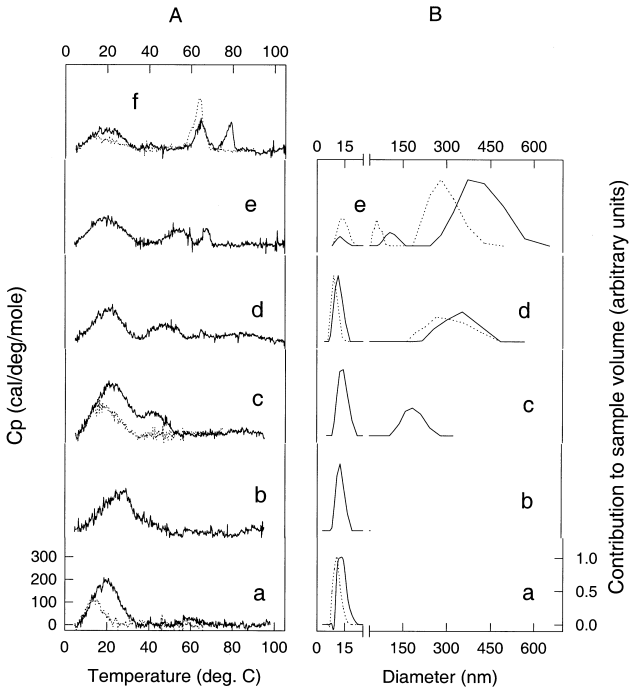

Fig. 5. Calorimetry and dynamic light scattering data from aqueous dispersions of mixtures Cer/GM1. Excess heat capacity vs. temperature (A) and contribution to sample volume vs. diameter (B) for pure GM1 (a), 3 mol% Cer (b), 5 mol% Cer (c), 20 mol% Cer (d), 27 mol% Cer (e) and 33 mol% Cer (f). In A, full lines represent the first DSC scan and dotted lines are reheat scans (see text); B shows light scattering before (full lines) and after (dotted lines) DSC scans of the same sample.

ments were observed upon leaving the samples for 24 h at room temperature or by diluting to lower concentrations.

The presence of Cer in different proportions induces marked changes of the mesomorphic behavior of GM1. In general, the thermotropic changes are shifted to progressively higher temperatures while the aggregated state shows increasing polidispersity with coexistence of large structures. Fig. 5Ab shows that the presence of only 3 mol% of Cer in the mixture shifts the position of the main peak from about 20°C to 28°C although the sample continues to contain only micelles, as seen in Fig. 5Bb. At 5 mol% of Cer in the mixture a broad shoulder shows up in the excess heat capacity vs. temperature scan, with a maximum excess heat capacity at approximately 42°C coexisting with the peak with a T_m at 22°C (Fig. 5Ac). In this sample dynamic light scattering reveals the presence of micelles representing about 70% of the total particle volume, with the usual distribution of sizes at 13.8 ± 2.2 nm, coexisting with larger structures that are more broadly distributed with diameters of 190 ± 30 nm and amounting to about 30% of the total particle volume (Fig. 5Bc). Both structures were still present after the temperature scan in the calorimeter, their size was slightly shifted downwards, but the proportion micelles/larger structures did not change.

At 15 mol% Cer in the mixture the T_m of the higher temperature component shifted further upwards (45°C) while the peak mostly contributed by GM1 micelles remained with a T_m of 22°C (not shown). In this sample the proportion of micelles remained similar to that of the sample with 5 mol% Cer, at 73–77% of the total particle volume, with an average diameter of 15 ± 3 nm (not shown). The amount of larger structures represented 23–27% of the total volume, with diameters of 300 ± 40 nm. Neither the diameters nor the volume contributions changed significantly with the successive calorimetry runs.

Mixtures with 20 mol% Cer showed again the peak at 22°C but with a reduced ΔH and C_{pmax} (Fig. 5Ad). The peak at higher temperature shifted upwards and centered at about 50°C. On a second run, the low temperature peak shifted to a lower T_m (17°C) with a decreased ΔH, and the second peak shifted to a higher T_m of 55°C (not shown). The light scattering revealed micelles of 14 ± 2 nm (70% volume contribution) and larger structures of 350 ± 44 nm (30% volume contribution) (Fig. 5Bd). After the calorimetry runs, both the micelles and the larger structures showed a slightly decreased size.

→

Fig. 6. Electron micrographs of representative samples. Electron micrographs of GM1 (a,e) and mixtures with 5 mol% Cer (b,f), 20 mol% Cer (c,g) and 33 mol% Cer (d,h). The white bars in the insets indicate 100 nm (a,e–h), 200 nm (b), 500 nm (c) and 1 μm (d). The sample with 5 mol% Cer in f was dispersed in a 2% sodium phosphotungstate solution, in order to allow visualization of interlamellar spacings. All the other samples were stained with 2% uranyl acetate solution after preparation of the dispersion.

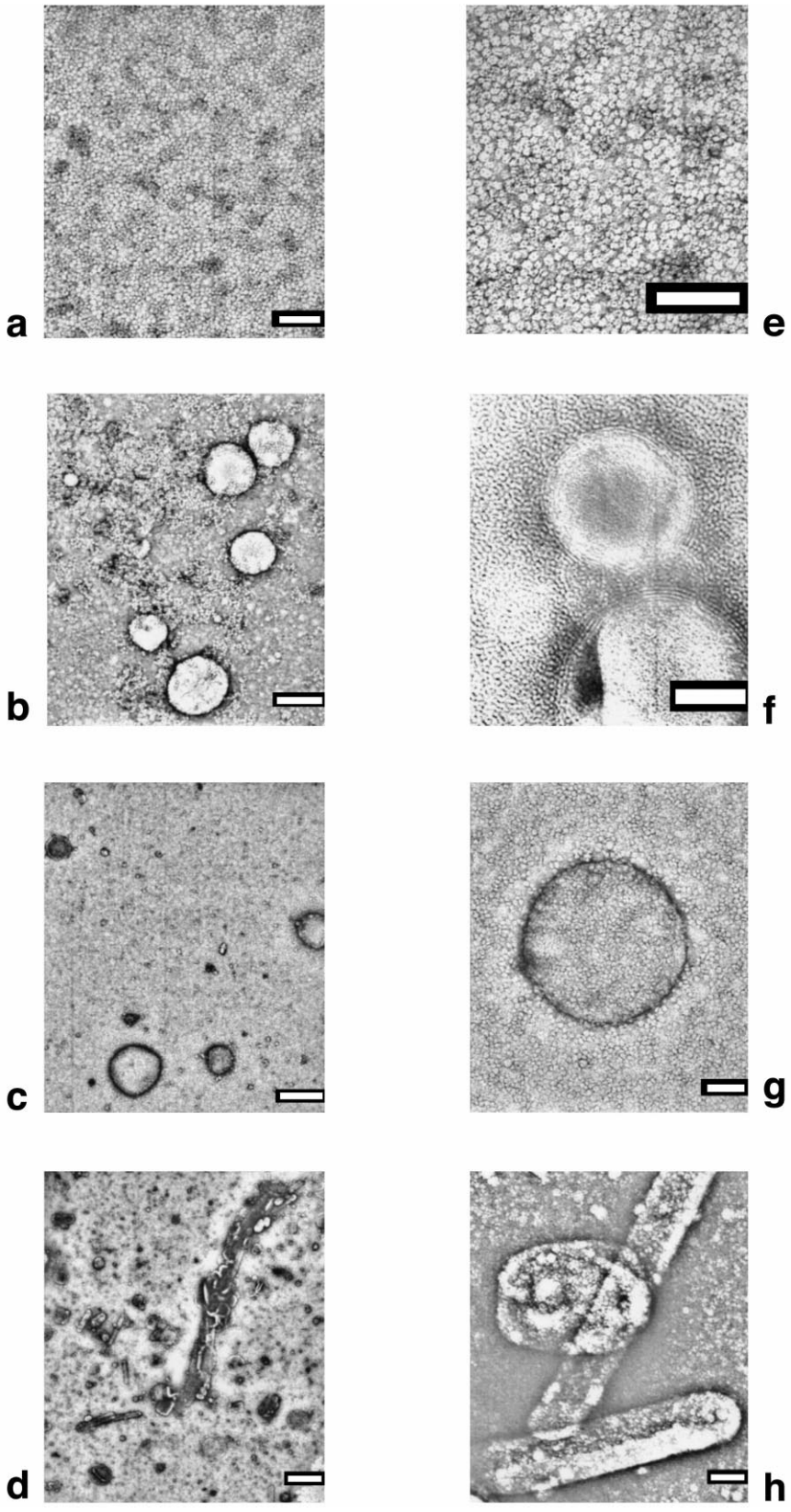
a
e
b
f
c
g
d
h

Calorimetry of the mixtures with 27 mol% Cer showed a peak at 20°C (the T_m of pure GM1), a peak at 58°C and a less reproducible peak at 65°C or 80°C (Fig. 5Ae). On cooling to 3°C, an immediate subsequent run showed a peak at 16°C (like when the sample of GM1 was re-run), a second peak at the same temperature than on the first run (58°C) and no transitions at 65°C or 80°C (not shown). Light scattering of this sample showed a complex size distribution, with at least three average sizes: 12.6 ± 2.4 nm (10% volume contribution), 110 ± 20 nm (15% volume contribution) and 400 ± 60 nm (75% volume contribution) (Fig. 5Be). After the calorimetric runs, the micelles remained at 14 ± 2 nm but contributed with 22% of the sample volume, while the larger structures were smaller than before running (60 ± 13 nm and 280 ± 60 nm) and contributed with 22 and 56% of the volume, respectively (Fig. 5Be).

In mixtures with 33 mol% Cer, the first calorimetric run showed peaks at 20°C (T_m of pure GM1), 65°C and 78°C (Fig. 5Af). On a second run, the GM1 peak was smaller with a T_m of 15°C, the peak at 78°C disappeared, and the peak at 65°C remained, but with increased ΔH and C_{pmax} (Fig. 5Af). Size distributions of this sample could not be resolved, apparently showing the presence of very large structures (2500 nm) and large polidispersity.

3.3. Electron microscopy

The electron microscopy observations confirmed that the 13 nm population observed by light scattering was constituted by micelles in the 9–15 nm range. These micelles were present in all the samples observed up to 33 mol% Cer (Fig. 6).

The samples containing 5 and 20 mol% Cer showed coexistence of micelles and multilamellar vesicles of increasing size (150–700 nm) and polidispersity as the concentration of Cer in the mixtures increased (Fig. 6b,c,f,g).

The 33 mol% Cer sample showed a large variety of structures present: micelles, vesicles of a wide range of sizes and long, thin tubular structures 100–400 nm in diameter and 0.545–2.620 μm long (Fig. 6d,h). The observed polidispersity probably accounts for the inability to reach a reasonable fit of the light-scattering measurements in this sample.

4. Discussion

4.1. Local molecular interactions in a plane interface

In mixed monolayers of Cer with dipalmitoylphosphatidylcholine it was previously shown that Cer preferably mixed with the liquid-expanded phase of the phospholipid. In these mixtures the liquid condensed character of Cer induced condensation of the liquid-expanded phase and abolition of the liquid-expanded to liquid-condensed surface pressure-induced phospholipid phase transition and its conversion to an abrupt transition between two liquid states [6].

The interface formed by ganglioside GM1 is of the liquid-expanded type over all values of surface pressure and Cer is miscible with it in all proportions (Fig. 1A). The interactions between Cer and ganglioside GM1 lead to non-ideal increases of the collapse pressure depending on composition, reduction of the mean molecular areas and decrease of the surface potential per unit of molecular surface density (surface potential/molecule) at all surface pressures. According to the molecular condensation, the intermolecular dispersion energies among Cer and GM1 are favorably increased at all surface pressures in the mixed film compared to an ideal mixture (Fig. 2). The surface compressibility modulus is a very sensitive parameter to detect slight changes of the monolayer phase state that can often go unnoticed in the surface pressure–molecular area isotherm [6]. The compressibility modulus of ganglioside GM1 reveals a very diffuse surface pressure-induced phase change gradually taking place between two liquid-expanded states under compression between about 90 and 70 $Å^2$ (Fig. 1B). Depending on the proportions of Cer the surface compressibility modulus progressively takes values, at comparable surface pressures, corresponding to liquid condensed states (Fig. 1B). The presence of Cer in small proportions (already noticeable below 5 mol%) condenses the film even at low surface pressures and abolishes the liquid phase change of GM1.

Condensation of the mean molecular areas and reductions of the surface potential/molecule in the mixed films may be due to interactions leading to decreases of the individual molecular parameters of both lipids or to a proportionally larger change in

mostly one of the components in the binary mixture; in addition, this may vary depending on the mutual proportions of the lipids in the monolayer. Which situation applies can be analyzed by inspecting the variation of the partial molecular areas and partial surface potential/molecule of each component in the mixed film [29,30]. Allowing for uncertainties in the estimation of the partial molecular parameters by the method of intercepts (values differing by about $\pm 10\%$ are not significant), Fig. 4 shows that the partial molecular area of GM1 at all surface pressures is progressively condensed starting at very low proportions of Cer and reaches, beyond a mole fraction of Cer of 0.6, values remaining at a relative plateau of about 30 $Å^2$. The latter is slightly lower than the closest possible packing limit for two parallel overcompressed hydrocarbon chains oriented perpendicularly to the monolayer interface [30]; for comparison, the limiting molecular area of Cer just before collapse is 38 ± 2 $Å^2$.

Due to its marked liquid-expanded character ganglioside GM1 can accommodate, up to high surface pressures, a rather large flexibility in the orientation and movement of the oligosaccharide chain [4] which contributes considerably to the perpendicular molecular dipole and thus to the surface potential/molecule

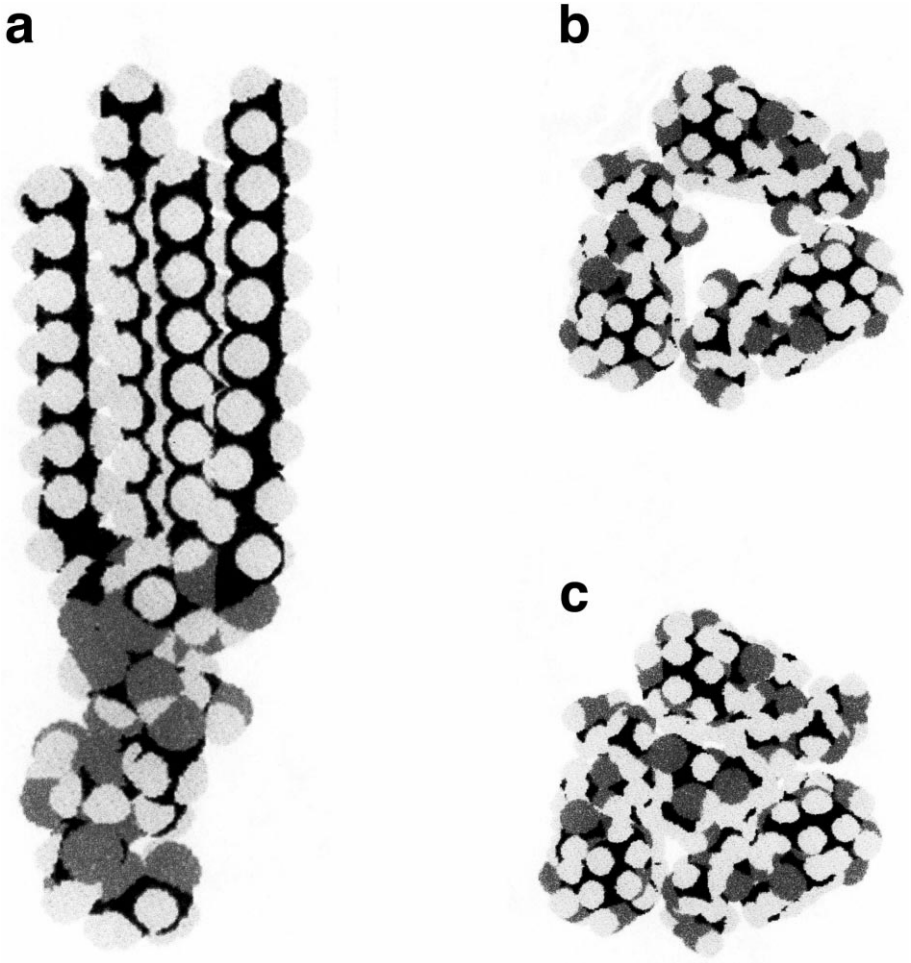

Fig. 7. Illustration of possible intermolecular arrangements in mixed monolayers of Cer and GM1. Space-filling molecular models in closely packed (i.e., above a surface pressure of 25 mN/m) monolayers of GM1 and Cer (a). End-up view as from the aqueous subphase of three closely packed molecules of GM1 without (b) or with (c) a molecule of Cer in the center. The models are in the optimal conformation after convergence of an energy minimization algorithm for torsion angles, interatomic bond stretching, angle and out-of-plane bending, and van der Waals interactions (Tripos Association, St. Louis, MO).

[7]. In agreement with this, the condensation induced by Cer on ganglioside GM1 appears mostly arising from the hydrocarbon portion of the molecule while the partial surface potential/molecule shows little variation over the range of composition where the partial molecular area of GM1 undergoes a reduction by more than 60%. Only when the packing area of GM1 is reduced to about its possible minimum value (above a mole fraction of Cer of 0.6) its partial surface potential/molecule abruptly decreases. This indicates that, at this composition of Cer and beyond, a marked reorientation of the oligosaccharide chain takes place leading to an abrupt depolarization of the ganglioside; in these films the partial surface potential/molecule of GM1 can even acquire a negative value in films enriched in Cer above a mole fraction of 0.9. At this proportions of Cer and above, GM1 molecules are likely to be completely surrounded and immersed in a fully condensed lattice of Cer. In this situation, the results suggest that ganglioside hydrocarbon chains become condensed to their minimum area with the oligosaccharide chains reduced in flexibility and stretched out into the aqueous phase perpendicularly to the interface contributing with an increased perpendicular dipole opposite to that of the hydrocarbon chains [7] leading to a marked molecular depolarization.

On the other hand, the partial molecular area of Cer, being already very condensed, appears only slightly affected by GM1, except at high mole fractions of the ganglioside above 0.7 (Fig. 4a). From this point the partial molecular area of Cer unrealistically decreases below the minimum value possible for two closely packed fully condensed hydrocarbon chains and, in mixtures with more than 90 mol% GM1, it shows negative values; this means that at these proportions of ganglioside Cer no longer contributes to the mean molecular area in the mixed monolayer. These results can be explained by the occurrence of 'molecular cavity effects' [30,36,37] whereby part or all of the molecular area contributed by one component in a mixed monolayer can apparently become 'hidden', sequestered into lateral surface defects brought about by the molecular packing of the other component. The existence of molecular cavity effects is in keeping with the variation of the surface potential/molecule with composition. Similar to the partial molecular area, this parameter shows that the dipolar properties of Cer do not vary much until the proportion of ganglioside GM1 in the film is very high (Fig. 4a). The invariance of both parameters for Cer up to a point were its proportions in the mixture are below 20 mol% entirely agree with the existence of molecular cavity effects for Cer in the mixed film with GM1. Fig. 7b,c illustrates these effects with molecular models and shows that, as indicated by the partial molecular area, at mole fractions of GM1 above about 0.75 it is possible to have enough 'cavities' in the lateral surface lattice so as to sequester molecules of Cer.

4.2. Thermotropic and topological behavior

The changes of the molecular packing parameters of Cer and GM1 are transduced to the average molecular geometry in the lipid interface, which are in turn amplified to the supramolecular structure of the self-assembled aggregate in bulk aqueous solution. Fig. 8 shows the theoretically expected variation of the critical packing parameter $P_c = v/a_o l_c$ for ideal mixtures with increasing proportions of Cer according to the cross-sectional mean molecular area at the hydrophobic-hydrophilic interface taken at two different surface pressures in monolayers (see [12,13]). It also shows the values obtained for P_c in representative real mixtures at defined proportions. Ganglioside GM1 self-assembles into more or less eccentric globular or cylindrical micelles with a $P_c = 0.42–0.47$ [12,13] while pure Cer should favor inverted micellar structures with $P_c = 1.22–1.27$ depending on variations of the lateral surface pressure.

In ideally mixed binary mixtures the condensed state of Cer induces a progressive reduction of the mean molecular area according to its proportions (see Fig. 2). This causes a gradual increase in the critical packing parameter of the mean ideally mixed molecule allowing values corresponding to progressively larger bilayer vesicles; at a mole fraction of Cer of about 0.7–0.8 (depending on the lateral surface pressure) the value of $P_c = 1$ is surpassed at which point the formation of inverted micellar structures (H_{II}- or cubic phase-type) should become possible in the ideal mixture (Fig. 8). The non-ideal interactions established between Cer and GM1 with increased condensation (see Fig. 2) lead to a larger value for P_c in the real mixtures (Fig. 8), for which a

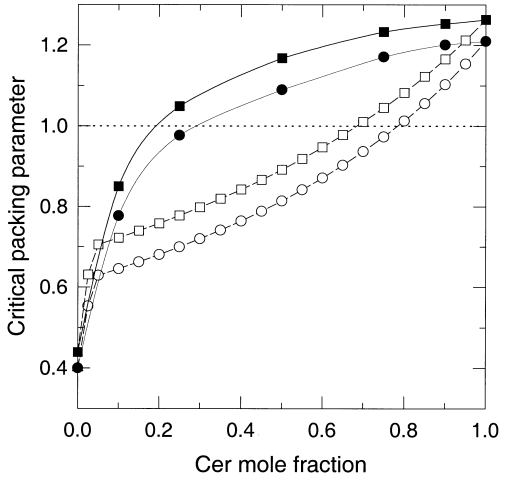

Fig. 8. Critical packing parameter calculated from monolayer data of Cer/GM1 mixtures. Critical packing parameter as a function of Cer mole fraction for ideal (hollow symbols) and real (filled symbols) mixtures at 10 mN/m (circles) and 30 mN/m (squares). The discontinuous line shows the limit for the possible formation of a non-bilayer (inverted micellar) phase.

marked departure from the micellar shape should be expected at smaller proportions of Cer than for ideally mixed molecules and larger, possibly non-bilayer structures should be expected above about 25 mol% of Cer in the mixture. Also, the condensation should favor lateral interaction among hydrocarbon chains and thus raise the phase transition temperature.

The results obtained in the calorimetric, dynamic light scattering and electron microscopy experiments are in full agreement with the local interactions observed in the mixed monolayers and with the expected variations of P_c with composition. In agreement with the condensation and favorably increased intermolecular interaction energies (see Fig. 3), the bulk aqueous dispersion of GM1 containing only 3 mol% Cer shows a marked shift of the T_m by about 8°C upwards. At 5 mol% Cer and above, the reduction in the mean molecular area, mostly due to a condensation of the ganglioside molecule (Fig. 4), determines a value for the critical packing parameter well in the range allowing the formation of bilayers (Fig. 8). In the mixture with 5 mol% Cer the calorimetric experiments reveal the presence of a component undergoing a phase transition centered at about 42°C and dynamic light scattering indicates that larger structures segregate out as a distinct population from the original micelles, while a proportion of the latter remain, probably represented calorimetrically by the component with the transition taking place at 22°C. Electron microscopy reveals the larger structures as multilamellar vesicles (Fig. 6b,f), thus confirming the formation of bilayers at this small amount of Cer in the mixture (5 mol%), and consistent with the predicted increase of cohesive intermolecular interaction energies.

At higher proportions of Cer the enhanced condensation induces the appearance of components with their phase transition progressively shifting upwards in temperature (Fig. 5A) while the contribution of the peak corresponding to the original micellar phase transition of GM1 decreases in importance; light scattering consistently reveals dispersions in which the volume contribution of large structures is increased. The composition ranges at which all these phase changes take place coincide with the proportions of Cer that cause condensations of mean molecular area in monolayers, leading to values of P_c in the range between 0.5 and 1 that allow formation of bilayer structures. Around 30 mol% Cer most of the sample lipid volume is contributed by large heterogeneous aggregates, namely, vesicles and long, thin tubular structures (Figs. 5B and 6d) and the mixtures with 27–33 mol% Cer show calorimetric transitions with higher transition temperatures (approaching the range of those exhibited by pure Cer, above about 70°C [32]) during the first run. These likely represent aggregates of Cer that are difficult to hydrate and containing GM1; in a second run the transition becomes more reproducible and its T_m is shifted downwards but still remains at rather high values just above 60°C (Fig. 5A) while the large and very large structures remain of the same size.

Acknowledgements

This work was supported by SECyT-UNC, CONICOR, FONCYT and CONICET, Argentina. The authors would like to thank Farm. Claudia Nome (IFFIVE-INTA) for her helpful assistance in electronic microscopy observations. D.C.C. is a postgraduate fellow and B.M. is Principal Career Investigator of CONICET.

References

[1] Y.A. Hannun, Functions of ceramide in coordinating cellular responses to stress, Science 274 (1996) 1855–1859.

[2] R.N. Kolesnick, F.M. Goñi, A. Alonso, Compartmentalization of ceramide signaling: physical foundations and biological effects, J. Cell Physiol. 184 (2000) 285–300.

[3] S. Hakomori, Bifunctional role of glycosphingolipids. Modulators for transmembrane signaling and mediators for cellular interactions, J. Biol. Chem. 265 (1990) 18713–18716.

[4] B. Maggio, The surface behavior of glycosphingolipids in biomembranes: a new frontier of molecular ecology, Prog. Biophys. Mol. Biol. 62 (1994) 55–117.

[5] D.A. Brown, E. London, Functions of lipid rafts in biological membranes, Annu. Rev. Cell Dev. Biol. 14 (1998) 111–136.

[6] D.C. Carrer, B. Maggio, Phase behavior and molecular interactions in mixtures of ceramide with dipalmitoylphosphatidylcholine, J. Lipid. Res. 40 (1999) 1978–1989.

[7] B. Maggio, The molecular electrostatics of glycosphingolipids in oriented interfaces, in: M.J. Allen, S.F. Cleary, A.E. Sowers, D.D. Shillady (Eds.), Charge and Field Effects in Biosystems, Vol. 3, Birkhauser, Boston, MA, 1992.

[8] G.D. Fidelio, B. Maggio, F.A. Cumar, Interaction of soluble and membrane proteins with monolayers of glycosphingolipids, Biochem. J. 203 (1982) 717–725.

[9] B. Maggio, J.M. Sturtevant, R.K. Yu, Effect of myelin basic protein on the thermotropic behavior of aqueous dispersions of neutral and anionic glycosphingolipids and their mixtures with dipalmitoylphosphatidylcholine, J. Biol. Chem. 262 (1987) 2652–2659.

[10] B. Maggio, R.K. Yu, Modulation by glycosphingolipids of membrane-membrane interactions induced by myelin basic protein and melittin, Biochim. Biophys. Acta 1112 (1992) 105–114.

[11] B. Maggio, I.D. Bianco, G.G. Montich, G.D. Fidelio, R.K. Yu, Regulation by gangliosides and sulfatides of phospholipase A2 activity against dipalmitoyl- and dilauroylphosphatidylcholine in small unilamellar bilayer vesicles and mixed monolayers, Biochim. Biophys. Acta 1190 (1994) 137–148.

[12] B. Maggio, Geometric and thermodynamic restrictions for the self-assembly of glycosphingolipid-phospholipid systems, Biochim. Biophys. Acta 815 (1985) 245–258.

[13] B. Maggio, J. Albert, R.K. Yu, Thermodynamic-geometric correlations for the morphology of self-assembled structures of glycosphingolipids and their mixtures with dipalmitoylphosphatidylcholine, Biochim. Biophys. Acta 945 (1988) 145–160.

[14] J.N. Israelachvili, D.J. Mitchell, B.W. Ninham, Theory of self-assembly of hydrocarbon amphiphiles into micelles and bilayers, J. Chem. Soc. Farad. Trans. II 72 (1976) 1525–1568.

[15] J.N. Israelachvili, S. Marcelja, R.G. Horn, Physical principles of membrane organization, Q. Rev. Biophys. 13 (1980) 121–200.

[16] J.M. Seddon, R.H. Templer, Cubic phases of self-assembled amphiphilic aggregates, Phil. Trans. R. Soc. Lond. 344 (1993) 377–401.

[17] L.C. van Gorkom, J.J. Cheetham, R.M. Epand, Ganglioside GD1a generates domains of high curvature in phosphatidylethanolamine liposomes as determined by solid state ^{31}P-NMR spectroscopy, Chem. Phys. Lipids 76 (1995) 103–108.

[18] M.M. Pincelli, P.R. Levstein, G.D. Fidelio, A.M. Gennaro, Cholesterol-induced alterations of the packing properties of gangliosides: an EPR study, Chem. Phys. Lipids 104 (2000) 193–206.

[19] M.A. Perillo, N.J. Scarsdale, R.K. Yu, B. Maggio, Modulation by gangliosides of the lamellar-inverted micelle (hexagonal II) phase transition in mixtures containing phosphatidylethanolamine and dioleoylglycerol, Proc. Natl. Acad. Sci. USA 91 (1994) 10019–10023.

[20] M.P. Veiga, J.L. Arrondo, F.M. Goñi, A. Alonso, Ceramides in phospholipid membranes: effects on bilayer stability and transition to nonlamellar phases, Biophys. J. 76 (1999) 342–350.

[21] B. Maggio, Control by ganglioside GD1a of phospholipase A2 activity through modulation of the lamellar-hexagonal (HII) phase transition, Mol. Membr. Biol. 13 (1996) 109–112.

[22] G. Basáñez, G.D. Fidelio, F.M. Goñi, B. Maggio, A. Alonso, Dual inhibitory effect of gangliosides on phospholipase C-promoted fusion of lipidic vesicles, Biochemistry 35 (1996) 7506–7513.

[23] A. Sáez-Cirión, G. Basáñez, G. Fidelio, F.M. Goñi, B. Maggio, A. Alonso, Sphingolipids (galactocerebroside and sulfatide) in lamellar-hexagonal phospholipid phase transitions and in membrane fusion, Langmuir 16 (2000) 8958–8963.

[24] G.D. Fidelio, T. Ariga, B. Maggio, Molecular parameters of gangliosides in monolayers: comparative evaluation of suitable purification procedures, J. Biochem. (Tokyo) 110 (1991) 12–16.

[25] M.L. Fanani, B. Maggio, Mutual modulation of sphingomyelinase and phospholipase A2 activities against mixed lipid monolayers by their lipid intermediates and glycosphingolipids, Mol. Membr. Biol. 14 (1997) 25–29.

[26] B. Maggio, T. Ariga, J.M. Sturtevant, R.K. Yu, Thermotropic behavior of glycosphingolipids in aqueous dispersions, Biochemistry 24 (1985) 1084–1092.

[27] L. Salem, Attractive forces between macromolecular chains of biological importance, Nature 193 (1962) 476–477.

[28] B. Maggio, F.A. Cumar, R. Caputto, Interactions of gangliosides with phospholipids and glycosphingolipids in mixed monolayers, Biochem. J. 175 (1978) 1113–1118.

[29] P.W. Atkins, Physical Chemistry, Oxford University Press, London, 1990.

[30] B. Maggio, T. Ariga, R.O. Calderon, R.K. Yu, Ganglioside GD3 and GD3-lactone mediated regulation of the intermolecular organization in mixed monolayers with dipalmitoylphosphatidylcholine, Chem. Phys. Lipids 90 (1997) 1–10.

[31] G.D. Fidelio, B. Maggio, F.A. Cumar, Molecular parame-

ters and physical state of neutral glycosphingolipids and gangliosides in monolayers at different temperatures, Biochim. Biophys. Acta 854 (1986) 231–239.
[32] J. Shah, J.M. Atienza, A.V. Rawlings, G.G. Shipley, Physical properties of ceramides: effect of fatty acid hydroxylation, J. Lipid Res. 36 (1995) 1945–1955.
[33] L. Cantu, M. Corti, E. Del Favero, E. Digirolamo, S. Sonnino, G. Tettamanti, Experimental evidence of a temperature-related conformational change of the hydrophilic portion of gangliosides, Chem. Phys. Lipids 79 (1996) 137–145.
[34] M. Hirai, T. Takizawa, S. Yabuki, Y. Nakata, K. Hayashi, Thermotropic phase behavior and stability of monosialoganglioside micelles in aqueous solution, Biophys J. 70 (1996) 1761–1768.
[35] D. Orthaber, O. Glatter, Time and temperature dependent aggregation behaviour of the ganglioside GM1 in aqueous solution, Chem. Phys. Lipids 92 (1998) 53–62.
[36] D.O. Shah, Surface chemistry of lipids, Adv. Lipid Res. 8 (1970) 347–431.
[37] B. Maggio, J.A. Lucy, Studies on mixed monolayers of phospholipids and fusogenic lipids, Biochem. J. 149 (1975) 597–608.